Finite Control Set Model Predictive Control-A Powerful Control Algorithm for Grid-Connected Power Converters

Mahlagha Mahdavi Aghdam[1], *Student Member, IEEE*, Li Li[1], *Member, IEEE*,
Jianguo Zhu[1], *Senior Member, IEEE*, and Omid Palizban[2]
[1]Centre of Green Energy and Vehicle Innovation, University of Technology Sydney, Ultimo, NSW 2007, Australia
[2] Department of Electrical and Energy Engineering, University of Vaasa, Vaasa FI-65101, Finland
Mahlagha.MahdaviAghdam@student.uts.edu.au

***Abstract*—This paper presents a detailed description of Finite Control Set Model Predictive Control applied to power converters. Some key features related to this methodology are presented and compared with model predictive control based space vector modulation methods. The basic models, principles, control diagrams, and simulation results are presented to provide a comparison between them. The analysis is performed on a three-phase/ two-level voltage source inverter, which is one of the most common converter topologies used in industry. Among the conclusions are the feasibility and great potential of Finite Control Set Model Predictive Control due to the advanced signal-processing capability, particularly for power systems with a reduced number of switching states and more complicated principles.**

Keywords—Distributed Generation; Grid-Tied Power Converter; Model Predictive Control; Space Vector Modulation;

I. INTRODUCTION

The raising number of Distributed Generation (DG) claims new strategies for the operation and management of the grid to sustain or enhance the power quality and reliability. The power electronic technology plays a key role in industrial applications such as integration of Renewable Energy Sources (RESs) into the grid. Power electronics have gone through a fast development, generally due to advances in power-semiconductor switches along with high performance control algorithms [1]. Therefore, to achieve high performances, converter topologies, modulation strategies, grid synchronization schemes, and control algorithms should be considered. The control structure of a grid connected converter is generally divided into two control loops. The outer control loop is dedicated to adjust the dc-link capacitor voltage. The inner one concentrates on either tracking the current or instantaneous active and reactive power references. In both scenarios, indirect control approaches, including the space vector modulation scheme, have been applied. Although these methodologies bring some benefits, complex coordinate transformation is required and much regulation effort is essential to guarantee the system stability [2].

Direct Power Control (DPC) pursues to control a power converter by employing the active and reactive powers as control variables. The conventional DPC is based on similar concepts as Direct Torque Control (DTC) for the motor drives [3]. DPC has turned into one of the popular control strategies due to its simplicity, outstanding transient performance, and robustness. Although DPC directly selects the power switch states to follow the desired active and reactive powers, the resulting switching frequency is varying [4-6].

Predictive algorithms have also been engaged to overcome the varying switching frequency problem of the DPC strategy. The Model Predictive Control (MPC) is able to work with system nonlinearities and constraints instantaneously. Besides, MPC can be applied easily in Multiple Input-Multiple Output (MIMO) systems as well as single Input-Single Output (SISO) systems. Yet, a precise system model is an essential to apply MPC.

MPC techniques applied to Power Electronics can be classified into two types: Finite Control Set MPC (FCS-MPC) and Continuous Control Set MPC (CCS-MPC). In the FCS-MPC approach, it takes benefit of the limited number of switching states of the power converter to solve the optimization problem. Alternatively, in the CCS-MPC a modulator produces the switching states from the continuous output of the controller [7]. In general, MPC evaluate, at each sampling instant, an optimal control problem over a finite prediction horizon. This optimization obtains an optimal control sequence for the whole prediction window. Succeeding to the receding horizon principle, only the first control act of this optimal sequence is applied to the system. At each sampling instant, this procedure is repeated using new state estimations or measurements [8].

This paper presents a description of FCS-MPC applied to grid-connected DC/AC power converter, which provides an optimization method to control the active and reactive powers. The MPC operating principle is introduced in Section II. A Two-Level three-phase Voltage Source Inverter topology is employed to implement MPC, in Section III. Section IV shows model predictive control based on Space Vector Modulation (MPC-SVM) for a three-phase inverter using direct power control and SVM switching strategy. The performance comparison of MPC versus MPC-SVM control techniques is presented in Section V. Finally, Section VI is devoted to the conclusion.

II. FCS-MPC Operating Principle

A. FCS-MPC Algorithm

Finite Control Set Model Predictive Control (FCS-MPC) takes the advantage of the discrete nature of power converters to moderate the MPC calculations with reduced computation time. As there are finite numbers of switching states in a converter, the prediction procedure will be selected through minimizing the cost function. Fig. 1 shows the main features of this control scheme.

Assuming that the state variables $x(k)$ is obtainable through measurement and estimation, which provides the current plant information, at the sampling instant k, $k > 0$, the current state variable $x(k)$ is used to predict its future values. In one sampling time ahead, the predicted state $x_{Pi}(k+1)$ can be obtained based on a prediction function f_P for each possible control set $S_i, i = 1,\dots,n$ as follows,

$$x_{Pi}(k+1) = f_P\{x(k), S_i\}, \qquad for\ i = 1,\dots,n\ .$$

where S_i is the i-th control set. A cost function f_J can be defined to select the optimal control set, based on the desired reference value x^*, as follow,

$$J_i = f_J\{x^*(k+1), x_{Pi}(k+1)\}, \qquad for\ i = 1,\dots,n.$$

The sampling time, T_s, is small enough in comparison with the system dynamic behaviour, hence the future reference value, $x^*(k+1)$, is anticipated to be same as the actual value, $x^*(k)$. In other words, the reference is assumed to be constant over T_s. The assessment of the cost function with the n predictions will cause n different costs. Certainly, the control action will be chosen as the one which leads to the minimum cost (min $\{J_i\}$, for $i = 1,\dots,n$). A typical representation for cost function J_i would be the error between the predicted value and the reference,

$$J_i = \|x^*(k+1) - x_{Pi}(k+1)\| \qquad (1)$$

The error in one sampling period is defined by (1) which can be calculated as an absolute value, square value or integral value. Although, the absolute error and squared error give similar results when a single-term cost function is used, squared error grants a better tracking when the cost function includes additional terms. The choice of cost function is one of the most important stages in the design of an MPC, since it allows not only to select the control objectives of the application, but also to include any required constraints. For example, in FCS-MPC, switching losses can be controlled by adding another term to the cost function J_P. Lastly, the optimal switching state (S_{opt}) that minimizes the cost function will be nominated as the next switching state [2].

To further show how the algorithm works, Fig. 2 shows the system behaviour in time and space vector representations, respectively. Based on the case in Fig. 2, the predicted value $x_{P2}(k+1)$ is the closest to the reference $x^*(k+1)$; therefore, S_2 is the optimum vector and applied at the sampling time *k*. Subsequently the same principle applies, that is, S_3 is selected and applied at the sampling time *k+1*. In the ideal theoretical case, we assume the variables can be measured, predicted, and controlled instantly at the sampling time *k*. However, it is not realizable in real-time applications, and this problem can be overcome if a one-step-delay is considered.

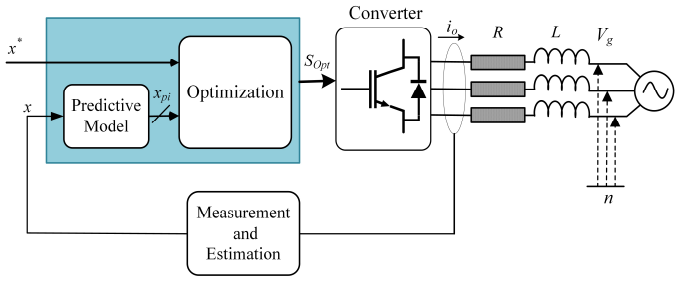

Fig. 1. FCS-MPC block diagram for grid-tied converter

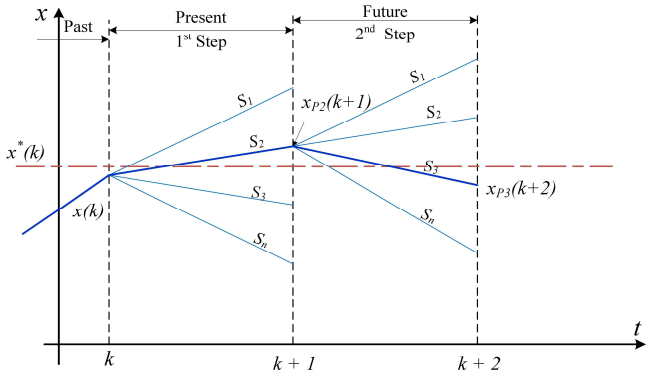

Fig. 2. Theoretical operating principle of FCS-MPC

B. FCS-MPC Challenges

As stated before, different variables can be involved in a cost function. They can even have different natures or units (active and reactive powers, current, voltage, switching losses, etc.). Since some variables have completely different values than others, this can cause coupling effects or to variations in the significance of one variable than the others in the cost function. A straightforward way to address this issue is to add a coefficient or weight factor for each variable in the cost function. The method of finding weighting factor is only empirical (i.e. try and error). Another approach for compensating the unit difference is normalizing each component (per unit value) in order to eliminate their unit effects.

Moreover, in terms of prediction horizon, there is no theoretical boundary to the number of predictions that can be executed. It is anticipated that with longer prediction horizon, more knowledge of the system is reflected in the cost function. Nevertheless, practical implementations are restricted by the

computational requirements of the algorithm, which will enforce a maximum number of achievable predictions [9-11].

III. Modeling the System

The two-level three-phase voltage source inverter (2L-3P VSI) is one of the most common converter topologies used in industry. Additionally, it depicts a general arrangement and operating principle that can be simply applied to other converter topologies. Hence, 2L-3P VSI is selected in this paper to describe the basic principles of MPC in power electronics applications.

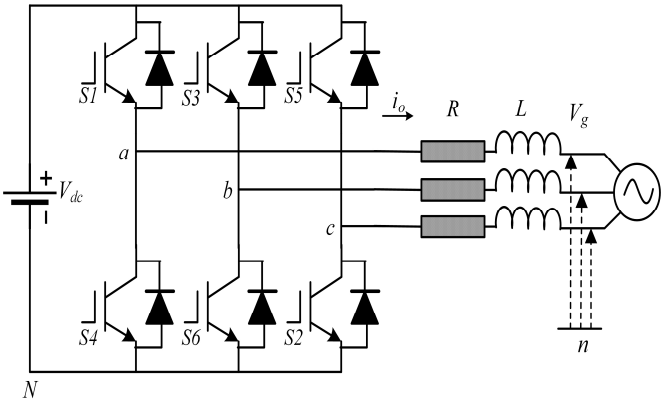

Fig. 3. Two-level / three-phase grid-tied inverter

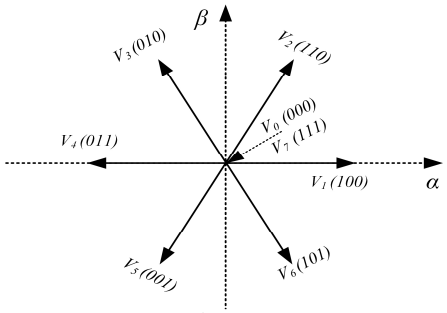

Fig. 4. The states of an inverter output voltage

A. Model of Grid-Tied Operation

The topology of a 2L-3P grid-tied VSI is illustrated in Fig. 3. It has six power switch-diode combinations, and IGBT has been selected as a power switch. For an n-phase m-level converter, the total number of possible switching states is m^n. Thus, eight possible switching states can be found for 2L-3P VSI. The output voltage space vectors generated by the inverter are defined by

$$V_i = \frac{2}{3}\left(V_{aN} + \alpha V_{bN} + \alpha^2 V_{cN}\right) \tag{2}$$

for $i = 1, \ldots, n$ where $\alpha = e^{j(\frac{2\pi}{3})}$. Then, by evaluating each of the switching states in (2), eight voltage vectors can be generated by the inverter, consisting of six active $(V1 - V6)$ and two zero $(V0, V7)$ voltage vector, as depicted in Fig. 4.

As space vector analysis is a good method in order to simplify three phase equations to a single equation, the mathematical equation of the grid-connected system will be

$$V_i = L\frac{di_o}{dt} + R.i_0 + V_g \tag{3}$$

where V, i_o and V_g represent the inverter terminal voltage, phase currents and grid voltage respectively. Then the state-space model can be written as

$$\frac{dx}{dt} = Ax + Bu \tag{4}$$

where,

$$x = [i_{o\alpha}\ i_{o\beta}\ V_{g\alpha}\ V_{g\beta}]^T \ , \ u = [V_{i\alpha}\ V_{i\beta}]^T \tag{5}$$

$$A = \begin{pmatrix} -\frac{R}{L} & 0 & -\frac{1}{L} & 0 \\ 0 & -\frac{R}{L} & 0 & -\frac{1}{L} \\ 0 & 0 & 0 & -\omega \\ 0 & 0 & \omega & 0 \end{pmatrix}, B = \begin{pmatrix} \frac{1}{L} & 0 \\ 0 & \frac{1}{L} \\ 0 & 0 \\ 0 & 0 \end{pmatrix} \tag{6}$$

Note that here V_g , i_o , and V_i are in the stationary transformation α-β frame (Clarke transformation). By discretizing the system state space model, the future value of output current can be estimated. Backward Euler method has been used for discretizing the plant [12, 13]. In this way, the future value of the system inputs is used to predict the future value of the controlled variables. If the system dynamics is described by:

$$\frac{dx}{dt} = f(x, u) \tag{7}$$

where *x* and *u* represent the controlled variable and input, then a backward Euler can be applied as

$$x(k+1) = x(k) + T_s\, f(x(k+1), u(k+1)) \tag{8}$$

B. Flexible Power Regulation

To help improve the system stability and power quality, flexible active and reactive power regulation have to be gained. Hence, the goal of MPC is to control the active and reactive powers. The MPC chooses the optimal voltage-vector sequence in order to control the power flow through the VSI. This strategy requires a predictive model of the instantaneous power evolution. In the stationary reference frame $\alpha - \beta$ and for a balanced three-phase system, instantaneous active and reactive powers injected into the grid by grid-connected inverter system can be defined as

$$\begin{pmatrix} i_{o\alpha}(k+1) \\ i_{o\beta}(k+1) \end{pmatrix} = \begin{pmatrix} i_{o\alpha}(k) \\ i_{o\beta}(k) \end{pmatrix} + \frac{T_s}{L}\left[\begin{pmatrix} V_{i\alpha}(k) \\ V_{i\beta}(k) \end{pmatrix} - \begin{pmatrix} V_{g\alpha}(k) \\ V_{g\beta}(k) \end{pmatrix} - R.\begin{pmatrix} i_{o\alpha}(k) \\ i_{o\beta}(k) \end{pmatrix}\right] \tag{9}$$

$$y = \begin{pmatrix} P(k+1) \\ Q(k+1) \end{pmatrix} = \frac{3}{2}\begin{pmatrix} V_{g\alpha} & V_{g\beta} \\ -V_{g\beta} & V_{g\alpha} \end{pmatrix}.\begin{pmatrix} i_{o\alpha}(k+1) \\ i_{o\beta}(k+1) \end{pmatrix} \tag{10}$$

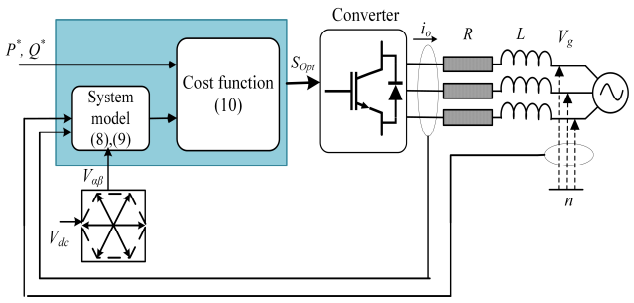

Fig. 5. Block diagram of flexible power flow

The block diagram of the direct power MPC in a 2L-3P VSI is depicted in Fig. 5. Moreover, the control algorithm of FCS-MPC is illustrated in Fig. 6. The current and grid voltage are measured at the same instant and used as the input for a predictive model that computes the values of P and Q at the next sampling time for each of the possible switching states of the inverter. The cost function is defined as

$$J = [P^* - P(k+1)]^2 + [Q^* - Q(k+1)]^2 \qquad (11)$$

The predictions are then evaluated so that the switching state, which minimizes the cost function, is applied to the converter.

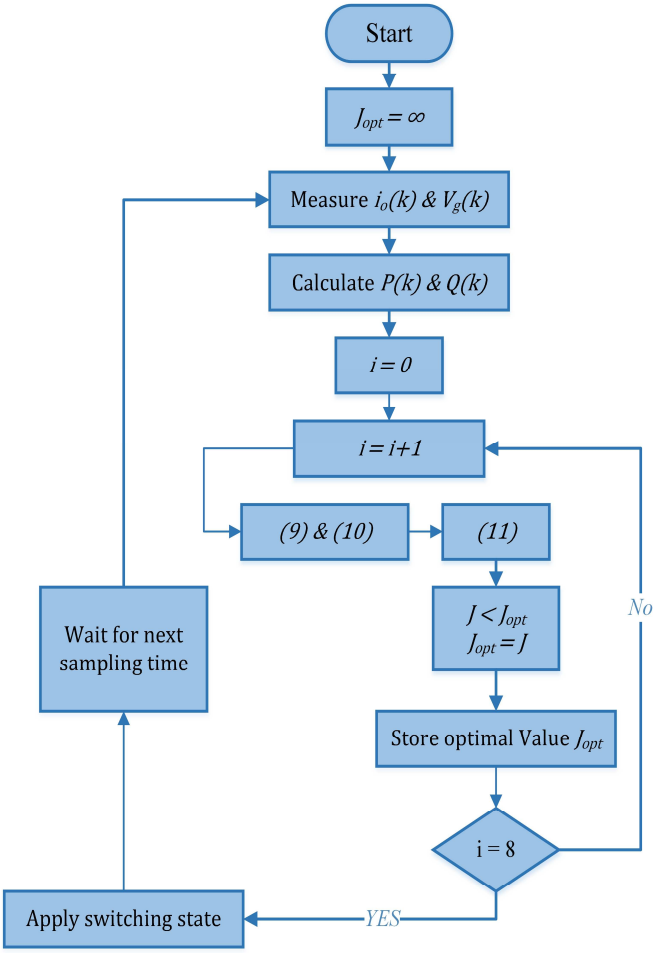

Fig. 6. FCS-MPC flowchart

TABLE I. Parameters of the System

Filter resistance	R	0.51Ω
Filter inductance	L	$4.8\ mH$
Grid voltage	V_g	$100\ V$
Dc source voltage	V_{dc}	$250\ V$
Voltage frequency	f	$50\ Hz$
Sampling period	T_s	$50\mu s$

C. *Simulation Results*

Simulations of a 2L-3P VSI with RL filter and load is carried out using MATLAB/Simulink and State-space model of the plan is discretized by selecting Backward Euler method. The model is shown in Fig. 6. The system parameters are listed in Table 1.

Fig. 7 illustrates the performance of controller. Initially the active and reactive powers are set to zero. While the active power reference is decreased from 0 to − 3 kW at 0.02 s and is back to 0 W at 0.04 s. After that, the active power reference is increased to 1 kW and then is kept at 0 W, whereas, reactive power reference is changed to -1, 0, and 1 kVAR respectively. It can be seen that the proposed MPC strategy presents excellent tracking.

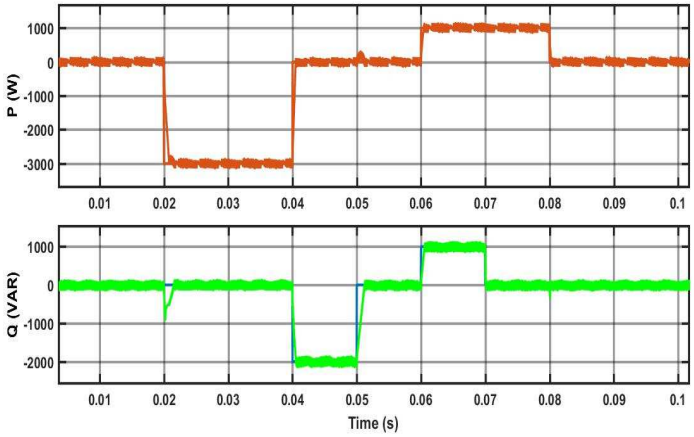

Fig. 7. Simulation results of FCS-MPC

IV. Model Predictive Control Based SVM

A. *Space Vector Modulation*

Space vector modulation (SVM) is an algorithm for the control of pulse width modulation (PWM). In the SVM technique, a reference voltage space vector V^* is provided, from which the switching patterns can be generated. The six non-zero voltage vectors ($V1 - V6$) can have the positions as shown in Fig. 8, forming a regular hexagon. With the six active vectors, the area between any two adjacent vectors is defined as a sector. The remaining two zero space vectors create no output voltage, and therefore they remain at origin in α-β plane defining no sector. At any time, V^* is estimated by two active space vectors and a zero pace vector (V_α^* and V_β^* components of V^* at angle θ).

TABLE II. Switching Pattern for Sector I

Switch	V_0	V_1	V_2	V_7	V_2	V_1	V_0
S_a	0	1	1	1	1	1	0
S_b	0	0	1	1	1	0	0
S_c	0	0	0	1	0	0	0

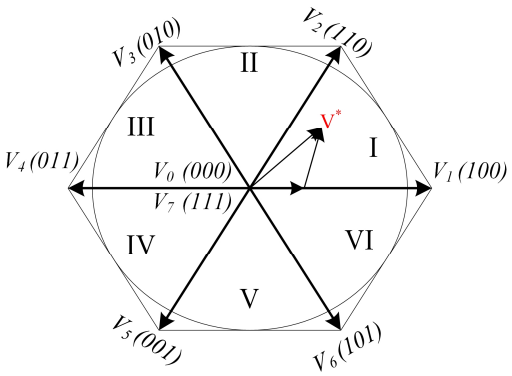

Fig. 8. Basic vectors and sectors

For example, as can be seen in Fig. 8, if V^* is in Sector I the voltage vector can be expressed as

$$T_1V_1 + T_2V_2 = T_s V^* \quad (12)$$

$$V^* = \sqrt{{V_\alpha}^2 + {V_\beta}^2} \quad (13)$$

$$\tan\theta = \frac{V_\beta}{V_\alpha} \quad (14)$$

where $(i-1)\frac{\pi}{6} < \theta < i.\frac{\pi}{6}$ for $i = 1,\ldots,n$ (number of sectors). Switching time durations T_0, T_1 and T_2 at any instant can be attained in (15-17) for $i = 1,\ldots,n$ as follow,

$$T_1 = \frac{\sqrt{3}|V^*|}{V_{dc}}\, T_s.\sin(\frac{i}{3}\pi - \theta) \quad (15)$$

$$T_2 = \frac{\sqrt{3}|V^*|}{V_{dc}}\, T_s.\sin(\theta - \frac{i-1}{3}\pi) \quad (16)$$

$$T_0 = T_s - T_1 - T_2 \quad (17)$$

The order of ON and OFF of the top three switches should satisfy the following principle: only one of the top three switches can change the switching status, for change of one basic voltage vector to another vector. The VSI will switch six times in one cycle. For example, given the voltage vector V^* in Sector I as shown in Fig. 8, V^* is made up of vectors $V_0, V_1, V_2, V_7, V_2, V_1$ *and* V_0. Corresponding switch S_a, S_b, S_c values and switching function waveforms for Sector I are shown in Table II and Fig. 9.

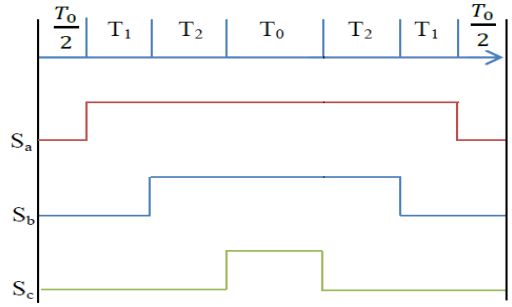

Fig. 9. Switching signals in Sector I

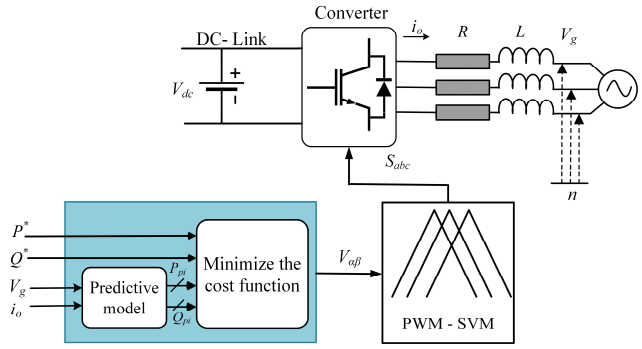

Fig. 10. The block diagram of MPC-SVM

B. A Combined MPC-SVM *Algorithm*

The objective of this section is to present a direct power control scheme of three-phase inverter based on a combination of MPC and SVM (MPC-SVM) approaches. The MPC technique operates with constant switching frequency SVM. For this purpose, an MPC principle is developed to calculate the required inverter average voltage vector, to be generated during each switching period T_S, to cancel out both active and reactive power tracking errors at the end of each sampling period. The computed inverter average voltage vector, in $\alpha - \beta$ reference frame, is converted into a sequence of switching states (adjacent voltage vectors) by means of SVM technique.

The MPC-SVM based power control block is shown in Fig. 10. At the beginning of each sampling time T_s, the inverter voltage vector is computed. After that, SVM method is used to generate a sequence of inverter switching states, to attain the control objective with constant switching frequency. This technique has no need for a PI controller. SVM, compared to conventional Sinusoidal PWM method, has optimum switching patterns and good dc-link voltage setup. The cost function (10) is used for minimizing the error between the predicted output and reference. The optimal value of cost function is determined and the corresponding control action, $V(k)$, from the control action set, V = [000 001 010 011 100 101 110 111], is applied across VSI in the next sampling instant. Note that in each sampling period eight predictions are performed and eight cost functions are evaluated before selecting the control action, V, for the next sampling instant. This method has been applied for voltage source rectifiers (VSRs) in [14] .

C. *Simulation Results*

Based on the block diagram of MPC-SVM, the model of MPC-SVM control system in Fig.10 is built in MATLAB/SIMULINK environment and the parameters used in this simulation are tabulated in Table 1. The discrete-time model of the plant is used to predict the behaviour of the voltage reference vector. Fig. 11 shows the performance of MPC-SVM controller. To improve the performance, the model should be estimated more accurately. Note that the

performance of MPC-SVM is sensitive to the parameters of load and filter, particularly to the filter inductance.

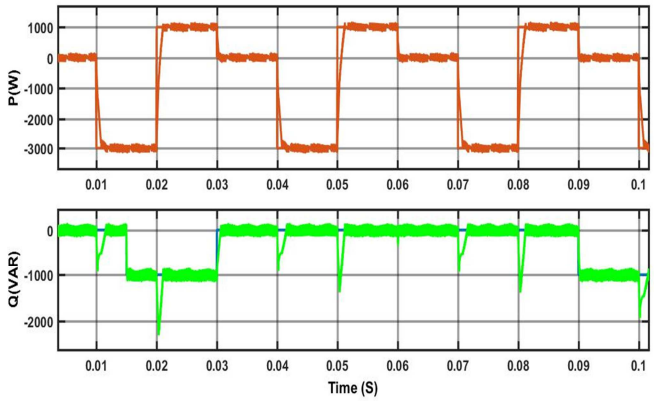

Fig. 11. Simulation results of MPC-SVM

V. Comparison

MPC controller selects the most appropriate voltage vector based on a cost function rather than a look-up table. Voltage-orientation direct power control could not achieve the same performance even if the sampling rate is higher. Unity power factor can be achieved by both methods but FCS-MPC is able to track the reference more accurately, as shown in Fig. 12.

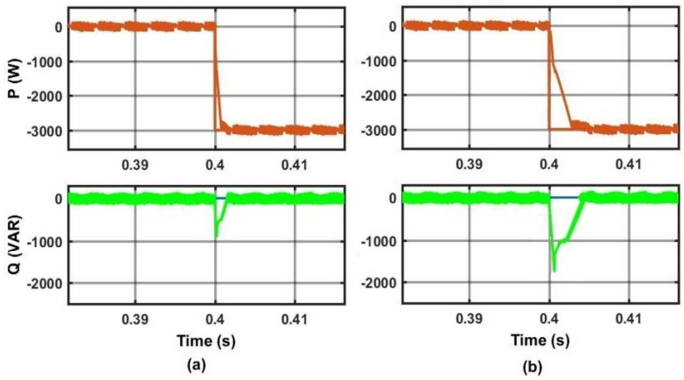

Fig .12. Simulation results for unity power factor (a)FCS-MPC (b)MPC-SVM

VI. Conclusion and Future Work

In this study, a model predictive control based finite control set technique is applied to a voltage source inverter with DPC strategy. It can reduce the enormous calculations in the online implementation of MPC. The simulation results show the proposed method leads to the good performances of the power tracking ability in both steady and transient state. The proposed control strategy can be used as a general control approach for distributed generation units to achieve grid-tied operation. By changing the cost function properly, different control objectives can be fulfilled.

As a broad conclusion, the MPC-DPC approach could become an alternative of voltage oriented control techniques for line-connected converters. This control method is powerful and is able to control various types of converter topologies and variables without the need of additional modulation techniques or internal cascade control loops. FCS-MPC takes the benefit of the discrete nature of power converters and advancement of the microprocessors in order to reduce the amount of calculations. For the future work, improving power quality and system stability through multi-objective cost function will be investigated. Furthermore, long prediction horizons will be explored. It is expected to decrease the power ripples considerably for adequate long horizons.

References

[1] J. M. Carrasco, L. G. Franquelo, J. T. Bialasiewicz, E. Galván, R. C. P. Guisado, M. Á. M. Prats, *et al.*, "Power-electronic systems for the grid integration of renewable energy sources: A survey," *Industrial Electronics, IEEE Transactions on,* vol. 53, pp. 1002-1016, 2006.

[2] S. Vazquez, A. Marquez, R. Aguilera, D. Quevedo, J. Leon, and L. G. Franquelo, "Predictive Optimal Switching Sequence Direct Power Control for Grid-Connected Power Converters," *Industrial Electronics, IEEE Transactions on,* vol. 62, pp. 2010-2020, 2015.

[3] I. Takahashi and T. Noguchi, "A new quick-response and high-efficiency control strategy of an induction motor," *Industry Applications, IEEE Transactions on,* pp. 820-827, 1986.

[4] A. Baktash, A. Vahedi, and M. Masoum, "Improved switching table for direct power control of three-phase PWM rectifier," in *Power Engineering Conference, 2007. AUPEC 2007. Australasian Universities*, 2007, pp. 1-5.

[5] J. Hu, J. Zhu, and D. G. Dorrell, "In-depth study of direct power control strategies for power converters," *IET Power Electronics,* vol. 7, pp. 1810-1820, 2014.

[6] T. Noguchi, H. Tomiki, S. Kondo, and I. Takahashi, "Direct power control of PWM converter without power-source voltage sensors," *Industry Applications, IEEE Transactions on,* vol. 34, pp. 473-479, 1998.

[7] S. A. Larrinaga, M. A. R. Vidal, E. Oyarbide, and J. R. T. Apraiz, "Predictive control strategy for DC/AC converters based on direct power control," *Industrial Electronics, IEEE Transactions on,* vol. 54, pp. 1261-1271, 2007.

[8] T. Geyer and D. E. Quevedo, "Performance of multistep finite control set model predictive control for power electronics," *Power Electronics, IEEE Transactions on,* vol. 30, pp. 1633-1644, 2015.

[9] C. Xia, T. Liu, T. Shi, and Z. Song, "A simplified finite-control-set model-predictive control for power converters," *Industrial Informatics, IEEE Transactions on,* vol. 10, pp. 991-1002, 2014.

[10] D.-K. Choi and K.-B. Lee, "Dynamic Performance Improvement of AC/DC Converter Using Model Predictive Direct Power Control With Finite Control Set," *Industrial Electronics, IEEE Transactions on,* vol. 62, pp. 757-767, 2015.

[11] J. Hu, J. Zhu, G. Lei, G. Platt, and D. G. Dorrell, "Multi-Objective model-predictive control for high-power converters," *Energy Conversion, IEEE Transactions on,* vol. 28, pp. 652-663, 2013.

[12] P. Cortés, J. Rodríguez, D. E. Quevedo, and C. Silva, "Predictive current control strategy with imposed load current spectrum," *Power Electronics, IEEE Transactions on,* vol. 23, pp. 612-618, 2008.

[13] S. Kouro, P. Cortés, R. Vargas, U. Ammann, and J. Rodríguez, "Model predictive control—A simple and powerful method to control power converters," *Industrial Electronics, IEEE Transactions on,* vol. 56, pp. 1826-1838, 2009.

[14] A. Bouafia, J.-P. Gaubert, and F. Krim, "Predictive direct power control of three-phase pulsewidth modulation (PWM) rectifier using space-vector modulation (SVM)," *Power Electronics, IEEE Transactions on,* vol. 25, pp. 228-236, 2010.